COSMO-SKYMED VERY SHORT REPEAT-PASS SAR INTERFEROMETRY OVER RURAL AREAS: THE VAL D'AGRI AND POTENZA TEST CASES IN BASILICATA, ITALY.

Pietro Milillo[1,2,3], Daniele Perissin[4], Paul Lundgren[2], Carmine Serio[1]

1. School of Engineering, University of Basilicata, Potenza, Italy
2. Jet Propulsion Laboratory, California Institute of Technology, Pasadena, California, USA
3. Seismological Laboratory, California Institute of Technology, Pasadena, California, USA
4. Department of Civil Engineering, Purdue University, West Lafayette, Indiana USA

ABSTRACT

Over the last three decades interferometric synthetic aperture radar (InSAR) techniques have attained a fundamental role in surface deformation monitoring. The main importance is given by two key factors: the exploitement of rich SAR data archives and the development of processing techniques able to extract information from these datasets. InSAR time series techniques such as permanent scatterers (PS) or SBAS have proven capable of estimating displacements to with 1 mm precision for targets that show a stable electromagnetic signature. At the same time the availability of SAR constellations with a reduced revisit time, such as the X band COSMO-SkyMed (CSK) and TerraSAR-X/PAZ satellites, has reduced the minimum detectable deformation gradient between two neighboring points and improved the theoretical precision given for a network of selected stable pixels. Independently from the applied processing methodology, the main drawback at X-band is the shorter time interval to temporal decorrelation. This effect can be partially mitigated by a short repeat time acquisitions plan. A technique able to deal with distributed scatterers is fundamental for extending the spatial coverage of the coherent area. In this paper we analyze the potential of X-band COSMO-SkyMed short repeat pass interferometry over a rural area in the southern part of Italy for assessing the capabilities and limitations of the Quasi-PS (QPS) technique in an X-band non-optimal scenario.

Index Terms— InSAR, rural area, decorrelation, time-series analysis, Basilicata

1. INTRODUCTION

The ongoing development of constellations of Synthetic Aperture Radar (SAR) satellite with short repeat time acquisitions allows us to explore the behavior of earth processes and anthropogenic phenomena with an unprecedented temporal and spatial resolution [1,2]. Such improvement, from monthly to daily repeat times, sheds a new light on the dynamics of ongoing processes deforming the Earth's surface [3], allowing a better characterization of both seasonal and secular deformation trends. SAR interferometry (InSAR) has been widely used for detecting deformation due to these various mechanisms. InSAR is characterized by several limitations such as variable atmospheric signal delays, orbit errors and temporal and geometric decorrelations. To mitigate these errors and better resolve time-varying deformation signals multitemporal InSAR analysis techniques have been developed, such as persistent scatterers (PS) interferometry (PSI) [4] and small baseline subset (SBAS) interferometry [5].

Each single technique has its own advantages and limitations. Several approaches and combinations of these two different techniques have been developed in [6-9].

PSI has the advantage of using very large baseline InSAR pairs referred to a common master for estimating time series of deformation and height accuracy at scatterers with a stable elctromagnetic signature (ie. not affected by temporal and spatial decorrelation). A limitation is its lack of spatial coverage over natural terrains.

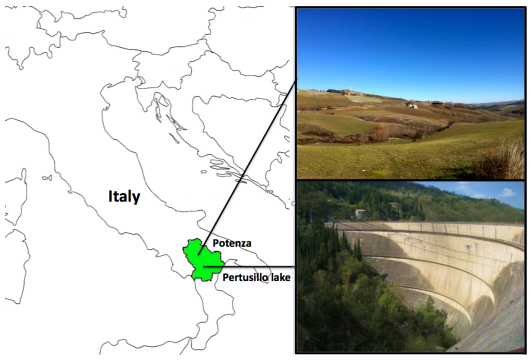

Fig. 1. Study area. Inset: (top) ground view of the rural area showing the scenario dominated by distributed scatterers. (bottom) Pertusillo dam located south the Agri valley.

The SBAS technique has the advantage of using a network of interferograms, estimating deformation at points that hold

The SBAS technique has the advantage of using a network of interferograms, estimating deformation at points that hold high spatial coherence in time (i. e. a group of temporarily coherent pixels given a certain set of temporal baselines). While not requiring a master image, SBAS-type techniques do require a reference date and pixel (or group of pixels). A limitation is the need for temporal network connectivity.

Independently from the InSAR time-series strategy used the main limiting factor for InSAR over rural areas is the temporal decorrelation [10]. The changing physical properties of the ground such as, reflectivity, soil moisture, land use and vegetation are the main cause of temporal decorrelation. Physically speaking rural areas can be defined as a group of distributed scatterers (DS) from which we can extract useful information after applying a spatial filter. As an example the simplest filtering operation that is commonly applied in SAR processing is multilooking. Besides changing parameters of the specific filter, the lower limit for retrieving useful information from DS is represented by the decorrelation time. This is a function of the radar wavelength and the physical properties of the soil and climatic parameters . After fixing the radar wavelength the only way to retrieve useful information from DS is reducing the minimum termporal sampling interval below the decorrelation time.

A recent analysis underestimates temporal decorrelation parameters using a direct inversion method mainly due to the lack of short-term interferometric combinations [11].

In this sense CSK provides a unique occasion for analyzing the effect of temporal decorrelation over rural areas at X-band (3 cm wavelength) with its non-uniform acquisition sampling (1,3,4,8,16 days and its multiple combinations). X-band is the less suitable wavelength for looking at DS because it is more sensitive to surface changes. In this paper we examine two test sites in southern Italy covering the Basilicata region, highlighting the impact of a short repeat time acquisition plan. Following a recently developed decorrelation model [11] we analyze the temporal decorrelation affecting the CSK dataset acquired with the full constellation (4 acquisitions very 16 days), showing how the QPS technique allows us to capitalize on the information present in distributed scatterers in areas where the PS approach typically fails. We also show the importance of short-repeat interval interferometry for monitoring the dynamics of deformation at the Pertusillo dam in Val D'agri, that is primarily driven by thermal induced deformation and the water hydrostatic pressure.

2. TECHNIQUE

In this section the fundamental concepts of the PS and Quasi-PS extension algorithm are reviewed. For further details, we refer the readers to [4], [8] and [11].

2.1. The PS and QUASI-PS technique

In both the PS and QPS techniques target height and velocity are estimated maximizing the phase coherence ξ of each selected pixel [4]. The main innovation in the QPS technique is the introduction of the spatial coherence γ as a weight in the estimation process. According to both techniques the formula becomes:

$$\xi_{PS} = \frac{\sum_{i=1}^{K} e^{-j\left(\Delta\phi_{H,p}^{i}+\Delta\phi_{V,p}^{i}-\Delta\phi_{p}^{i}\right)}}{K} \qquad (1)$$

$$\xi_{QPS} = \frac{\sum_{i=1}^{K} \gamma^{i} e^{-j\left(\Delta\phi_{H,p}^{i}+\Delta\phi_{V,p}^{i}-\Delta\phi_{p}^{i}\right)}}{\sum_{i=1}^{K} |\gamma^{i}|} \qquad (2)$$

Where $\Delta\phi_{H,p}^{i}$ and $\Delta\phi_{V,p}^{i}$ are the phase terms that depend on the target height and the deformation velocity and $\Delta\phi_{p}^{i}$ is the acquired interferometric phase compensated for flat terrain. K is the total number of interferograms used.

The main differences between the PS and QPS techniques are the pixel candidate selection, and the graph connecting in space and time all the acquisitions. In the PS technique initial candidate pixels are chosen within the pixels that exhibit an amplitude stability index above a given threshold (typically 0.8). The link network is arranged as a single master image interfering with all the slaves and only PS are processed without requiring interferogram generation.

The QPS technique candidate pixels are chosen according to the spatial coherence map of the single interferogram. The interferogram graph structure is based on a minimum spanning tree (MST) approach maximizing the normalized cross-correlation coefficient between two images. Theoretically every pixel could have a different interferogram network that maximizes its spatial coherence. The improvement of the QPS technique is the ability to include pixels affected by temporal or spatial decorrelation phenomena (i. e. distributed scatterers) at the expense of the spatial resolution reduced by the spatial averaging intrinsic to the coherence map generation process.

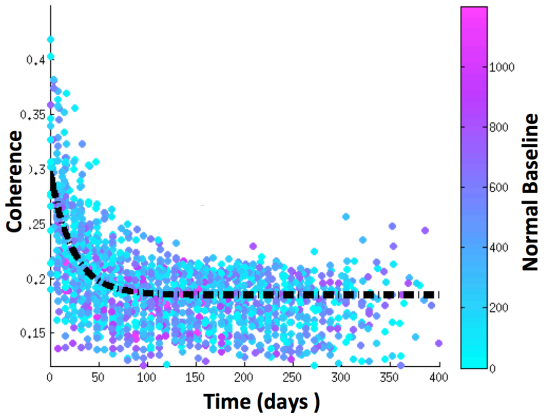

Fig. 2. Scatter plot of the estimated coherence versus temporal baseline. The average coherence as been calculated

over all the possible 1653 interferograms given 58 acquisitions.

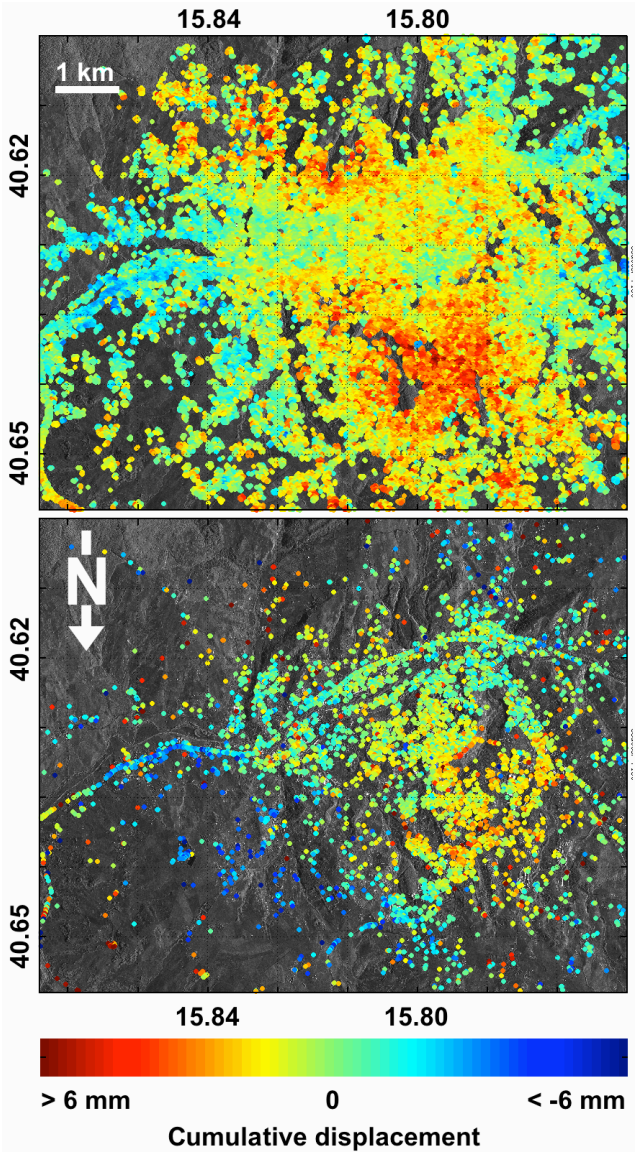

Fig. 3. Cumulative displacement maps (top) QPS (bottom) PS over Potenza town. The QPS using the full graph show landslide area already identified in [16] with ground based measurements.

2.2. Temporal decorrelation model

In order to optimize the MST and identify possible criticalities in the SAR dataset a temporal decorrelation model is required when looking at time-series analysis in rural areas. The practical utilization of these models is mainly related to the estimation of the decorrelation that is typical relative to the land use. For this purpose we adopt the temporal decorrelation model developed in [11]. This model, initially announced in [12] and [13], describes scatterers within a resolution cell as a two-state Markov chain random process where pixels assumes two different states: coherent or incoherent. A minimum coherence value γ_∞ and an initial coherence γ_0 is then introduced leading to:

$$\hat{\gamma}(t) = (\gamma_0 - \gamma_\infty)e^{-t/\tau} + \gamma_\infty \quad (3)$$

$$\tau = \frac{2}{\sigma_r^2}\left(\frac{\lambda}{4\pi}\right)^2 \quad (4)$$

Where σ_r is the variance of the motion of the scatterers in the line of sight direction and λ is the radar wavelength.
We found through a non-linear least squares approach that, on average, the entire scene is characterized by $\tau = 23.14 \pm 4$ days, $\gamma_0 = 0.29 \pm 0.02$ and $\gamma_\infty = 0.18 \pm 0.003$ (Fig.2). We found that this dataset is insensitive to geometrical decorrelation since all the pairs with normal baseline larger than 150 meters do not show a particularly different behavior if compared with shorter normal baseline pairs. Given the γ_0 and τ found for this particular dataset we expect that the QPS approach will significantly extend the analysis to distributed scatterers.

3. DATA PROCESSING

We processed 54 right-looking CSK ascending images acquired between September 2010 and February 2012 over Potenza in stripmap mode in VV polarization, at an off nadir angle of 43.5 degrees (beam HI_16). The PS and QPS processing have been performed using the SARPROZ algorithm [14]. The technique used in this analysis is a classical InSAR multitemporal processing method, in which we adopted a non-linear model of deformation in time [15]. For the QPS technique we consider a coherence estimation window of 3 by 3 pixels and a multilook factor of 10 in both the azimuth and range directions. We exploited the full graph composed of 1653 interferograms using 0.7 as the threshold for the coherence. For the PS technique we used as threshold of 0.78 for the amplitude stability index.

4. RESULTS

Figure 3 shows the cumulative displacement maps for the Potenza dataset calculated with both the PS and QPS techniques. About 20,000 PS where indentified versus 360,000 coherent pixels analyzed with the QPS algorithm. A 180% improvement of detected usable pixels allowed us to extend the spatial coverage of our analysis and highlight important features related to areas subject to landslides. We found a good agreement between our displacement map and the landslide inventory from [16]. In particular the QPS technique is able to better characterize the Varco D'Izzo landslide [17] whereas the PS technique showed only a few PS detected. Beside the improved spatial coverage, it is interesting to show how short repeat-pass interferometry

allows measurement of the dynamics of the seasonal deformation at the Pertusillo dam (Fig. 4). The deformation

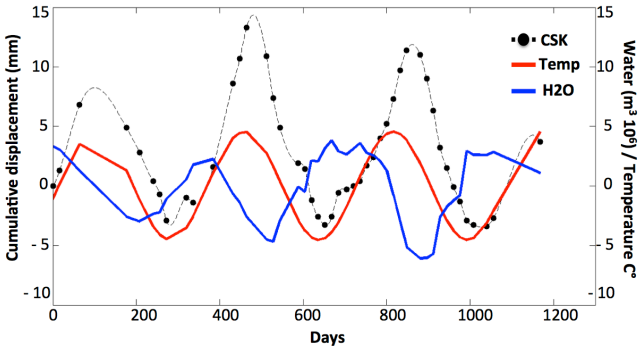

Fig. 4. Seasonal dynamics at the Pertusillo dam. The deformation recorded by CSK time-series is the superimposition of two separate seasonal effects related to the thermal dilation and hydrostatic pressure at the dam walls.

in this case is mainly driven by the temperature and the hydrostatic pressure of the water on the walls of the dam. The application of new stacking techniques together with short-repeat time interferometry looks promising for monitoring rural-areas and for measuring and identifying time-varying deformation processes.

5. ACKNOWLEDGEMENTS

COSMO-SkyMed data products processed at JPL under license from ASI as part of a collaborative project between CIDOT and University of Basilicata. Original COSMO··SkyMed product - ©ASI - Agenzia Spaziale Italiana - (2014-2015). Part of this research was supported by the NASA Earth Surface and Interior Focus Area and performed at the Jet Propulsion Laboratory, California Institute of Technology. The work of P. Milillo was done while he was a Special Student at Caltech. Any use of trade, product, or firm names is for descriptive purposes only and does not imply endorsement by the U.S. Government. We thank "Autorità Interregionale di Bacino della Basilicata" for the Pertusillo dam water levels.

6. REFERENCES

[1] Milillo, P.; Fielding, E.J.; Shulz, W.H.; Delbridge, B.; Burgmann, R., "COSMO-SkyMed Spotlight Interferometry Over Rural Areas: The Slumgullion Landslide in Colorado, USA," Selected Topics in Applied Earth Observations and Remote Sensing, IEEE Journal of , vol.7, no.7, pp.2919,2926, July 2014. doi: 10.1109/JSTARS.2014.2345664

[2] Milillo, P.; Riel, B.; Minchew, B.; Yun, S.; Simons, M.; Lundgren, P.; "On the synergistic use of SAR constellations data exploitation for Earth Science and Natural Hazard response," Selected Topics in Applied Earth Observations and Remote Sensing, IEEE Journal of , in Press.

[3] Riel, B.; Milillo, P.; Simons, M.; Lundgren, P.; Kanamori, H.; and Samsonov., S.,“ The collapse of Bárðarbunga caldera, Iceland “. Geophys. J. Int. (July, 2015) 202 (1): 446-453 doi:10.1093/gji/ggv157

[4] Ferretti, A.; Prati, C.; Rocca, F., "Permanent scatterers in SAR interferometry," Geoscience and Remote Sensing, IEEE Transactions on , vol.39, no.1, pp.8,20, Jan 2001. doi: 10.1109/36.898661

[5] Berardino, P.; Fornaro, G.; Lanari, R.; Sansosti, E., "A new algorithm for surface deformation monitoring based on small baseline differential SAR interferograms," Geoscience and Remote Sensing, IEEE Transactions on , vol.40, no.11, pp.2375,2383, Nov 2002. doi: 10.1109/TGRS.2002.803792

[6] Costantini, M.; Guglielmi, M.; Malvarosa, F.; Minati, F., "A Generalized Space-Time Formulation for Robust Persistent Scatterer Interferometry," Geoscience and Remote Sensing Symposium, 2006. IGARSS 2006. IEEE International Conference on , vol., no., pp.1240,1243, July 31 2006-Aug. 4 2006. doi: 10.1109/IGARSS.2006.320

[7] Hooper, A., P. Segall, and H. Zebker (2007), Persistent scatterer interferometric synthetic aperture radar for crustal deformation analysis, with application to Volcán Alcedo, Galápagos, J. Geophys. Res., 112, B07407, doi:10.1029/2006JB004763.

[8] Perissin, D.; Teng Wang, "Repeat-Pass SAR Interferometry With Partially Coherent Targets," Geoscience and Remote Sensing, IEEE Transactions on , vol.50, no.1, pp.271,280, Jan. 2012 doi: 10.1109/TGRS.2011.2160644.

[9] Ferretti, A.; Fumagalli, A.; Novali, F.; Prati, C.; Rocca, F.; Rucci, A., "A New Algorithm for Processing Interferometric Data-Stacks: SqueeSAR," Geoscience and Remote Sensing, IEEE Transactions on , vol.49, no.9, pp.3460,3470, Sept. 2011 doi: 10.1109/TGRS.2011.2124465

[10] R. Hanssen, Radar Interferometry: Data Interpretation and Error Analysis, vol. 2. Dordrecht, The Netherlands: Kluwer, 2001.

[11] Morishita, Y.; Hanssen, R.F., "Temporal Decorrelation in L-, C-, and X-band Satellite Radar Interferometry for Pasture on Drained Peat Soils," Geoscience and Remote Sensing, IEEE Transactions on , vol.53, no.2, pp.1096,1104, Feb. 2015. doi: 10.1109/TGRS.2014.2333814

[12] F.RoccaModelingInterferogramStacksIEEETrans. Geosci. Remote Sens. Vol 45, No. 10, Oct. 2007

[13] A. Parizzi, X. Cong, and M. Eineder, “First results from multifrequency interferometry. A comparison of different decorrelation time constants at L, C and X band,” in Proc. Fringe, Frascati, Italy, 2009, pp. 1–5.

[14] Perissin, D., Wang, Z., Wang, T., 2011. The SARPROZ InSAR tool for urban subsidence/manmade structure stability monitoring in China, In: Proceedings of ISRSE 2011, Sidney, Australia, 10–15 April.

[15] Ferretti A., Prati, C., Rocca, F. 2000. Nonlinear subsidence rate estimation using permanent scatterers in differential SAR interferometry. IEEE Transactions on , vol.38, no.5, pp.2202,2212, Sept 2000.

[16] Caniani, D., Pascale, S., Sdao, F., and Sole, A.: Neural networks and landslide susceptibility: a case study of the urban area of Potenza, Nat. Hazards, Springer (Ed.), 45, 55–72, 2008.

[17] Vallario, M.; Paterna, G.; Vassallo, R.; Di Maio, C.: Geometria di un esteso e complesso sistema franoso in argille varicolori. IARG 2011. (in Italian) 2011.